

## MECA Electrometer: Initial Calibration Experiments

M. Buehler, L-J. Cheng, O. Orient, and Michael Thelen  
Jet Propulsion Laboratory  
California Institute of Technology  
R. Gompf, J. Bayliss, and J. Rauwerdink  
Kennedy Space Flight Center  
National Aeronautics and Space Administration

### ABSTRACT

The Mars '01 lander contains an electrometer designed to evaluate the electrostatic nature of the Martian regolith (soil) and atmosphere. In this paper the initial calibration and response of the triboelectric sensors were measured between  $-60^{\circ}\text{C}$  and room temperature. The sensor has an electric field sensitivity of  $35\text{ kV/cm}\cdot\text{V}$  and room temperature drift of  $\sim 3\text{ }\mu\text{V/sec}$ .

**INTRODUCTION:** The electrometer is part of MECA (Mars Environmental Compatibility Assessment) project. The objective is to gain a better understanding of the hazards related to the human exploration of Mars. The electrometer will be built into the heel of the Mars '01 robot arm scoop as seen in Fig. 1. The electrometer operates over an 8-wire serial interface, is housed in a volume of  $\sim 50\text{ cm}^3$ , consumes less than 250 mW, and weighs  $\sim 50\text{ g}$ .

As seen in Fig. 1, the instrument has four sensor types: (a) triboelectric field, (b) electric-field, (c) ion current, (d) temperature. The triboelectric field sensor array contains five insulating materials to determine material charging effects as the scoop is dragged through the Martian regolith. The insulating materials will be chosen after Earth-based tests in Mars simulant soils.

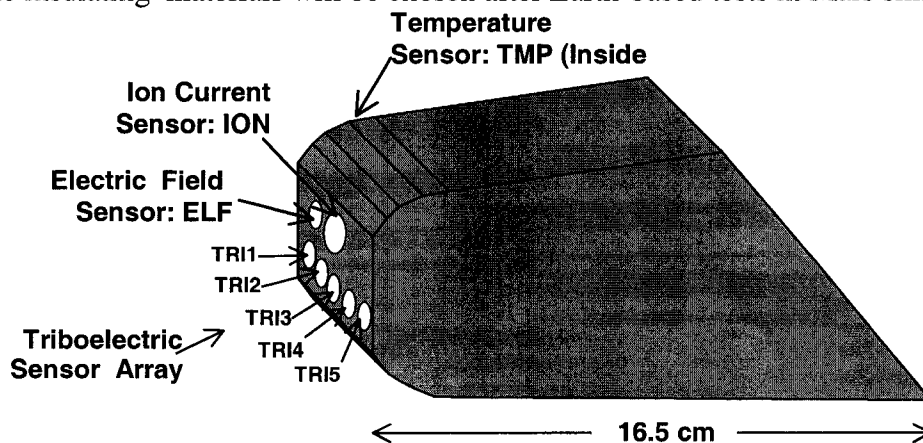


Figure 1. Electrometer sensor suite mounted in the heel of the Mars '01 scoop.

The engineering drawing of the scoop and the electrometer housing are shown in Fig. 2. During digging operation the electrometer is out of the way. After digging, the scoop is rotated so the electrometer head is pointing down toward the Martian soils allowing it to be rubbed against the Martian soil.

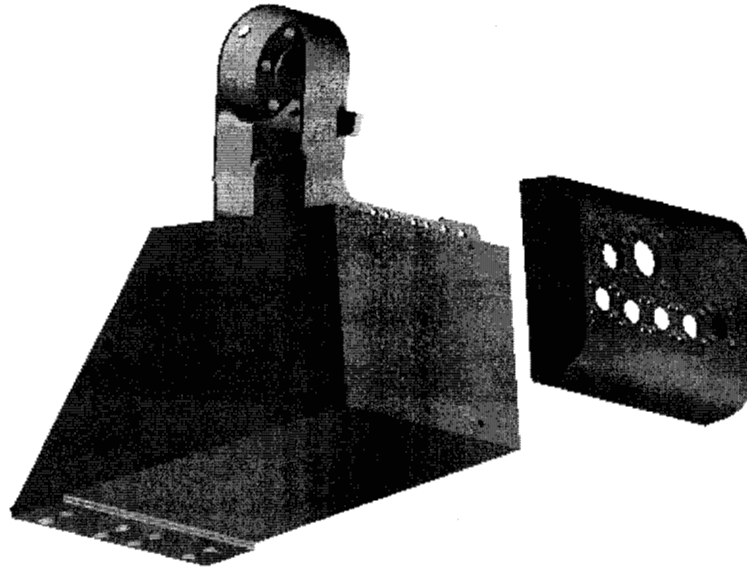


Figure 2. Electrometer titanium housing attached to back of aluminum scoop.

The scoop is located at the end of the robotic arm on the Mars 2001 lander as depicted in Fig. 3. The electrometer is part of the MECA project which has a material patch experiment to determine the effects of dust adhesion, a wet chemistry laboratory with ion selective electrodes to characterize the ionic content of the soil, and microscopy station with optical and atomic force microscopes to determine particle size and hardness.

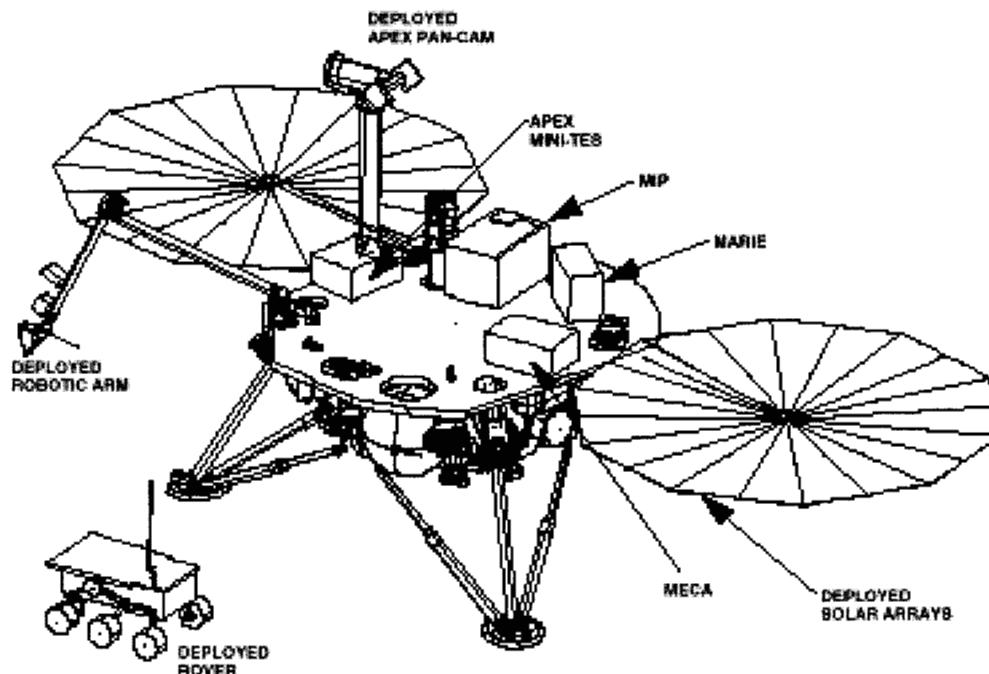


Figure 3. Overview of the Mars '01 lander. Some of the MECA experiments located in the box on the lander deck. The electrometer is located on the scoop on the robotic arm.

**OPERATION:** In the rubbing sequence, depicted in Fig. 4, the scoop is first lowered against the Martian soil. During the start of the traverse, the electrometer is zeroed by closing a switch which will be discussed later. After reaching the end of its traverse, the scoop is abruptly removed from the soil at which time the triboelectric sensor response, illustrated in the figure, is measured. The parameters and typical values for this operation are included in the figure caption.

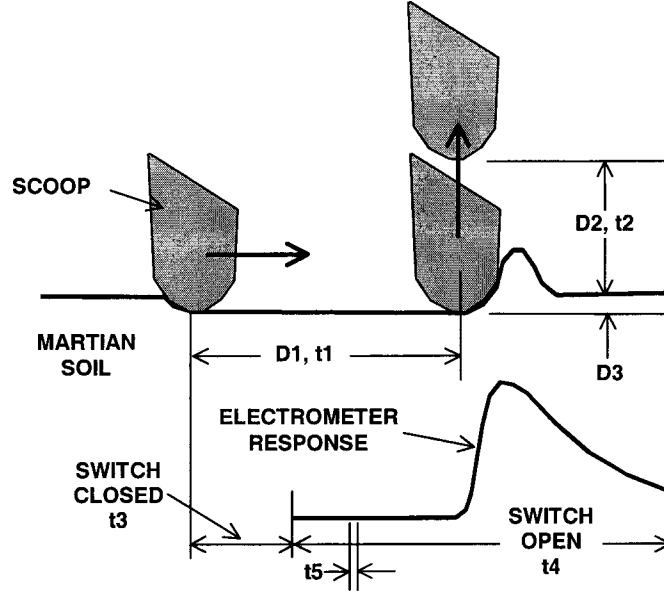


Figure 4. Operational scenario for the scoop where recommended operating parameters are:  $D1 = 10$  cm is the traverse distance,  $D2 = 1$  cm is the liftoff distance,  $D3 = 0.5$  to  $1$  cm is the penetration depth,  $t1 = 10$  s is the traverse time,  $t2 = 0.5$  s is the liftoff time,  $t3 = 1$  s is the switch close time,  $t4 = 19$  s is the data acquisition time, and  $t5 = 0.1$  s is the time between data points.

Physical insight into this process is illustrated in Fig. 5. As seen on the left, charge is generated triboelectrically across capacitor  $C3$  as the insulator is rubbed on the Martian surface.

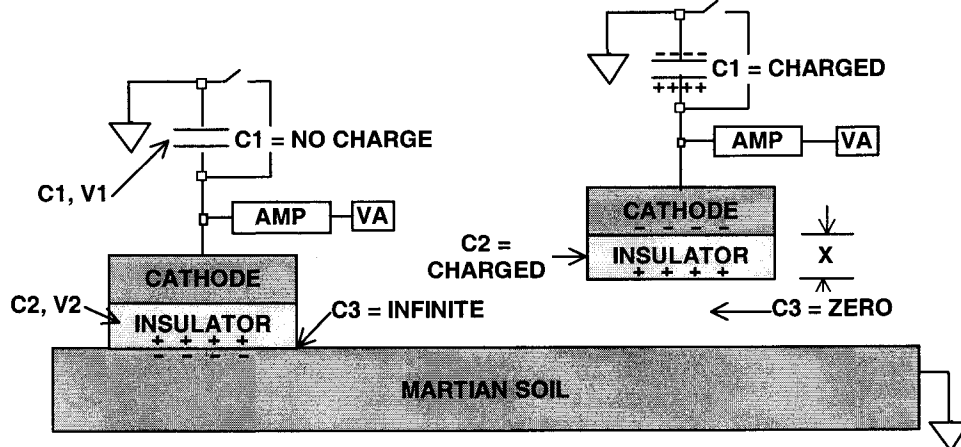


Figure 5. Charge distribution in the electrometer during rubbing (left) and after removal from the surface (right).

Since the charges are in close proximity across  $C3$ , no charge appears across capacitors  $C1$  or  $C2$ . As the insulator is removed from the surface, the charges redistribute themselves across  $C1$  and  $C2$  according to the charge relationship  $Q1 = Q2$  and provide the signal for the amplifier.

The sensitivity of the electric field developed across the insulator to the sensor output voltage is derived as follows. The charge relationship for the series capacitors,  $C1$  and  $C2$ , is  $Q1 = Q2$ . Given that  $Q1 = C1 \cdot V1$ ,  $Q2 = C2 \cdot V2$ ,  $C2 = \epsilon A/X$ , and  $E2 = V2/X$  it follows that  $E2 = (C1/\epsilon A) \cdot V1$  or that the amplifier input sensitivity is  $S1 = dE2/dV1 = C1/(\epsilon A)$  where  $\epsilon$  is the dielectric constant of the insulator and  $A$  is the area of the insulator. The amplifier output is related to it input via the amplifier gain,  $G$  or  $V1 = VA/G$ . A theoretical value can be calculated for  $S1$  from the component values. That is for  $C1 = 1 \text{ nF}$ ,  $A = 0.316 \text{ cm}^2$ , and  $\epsilon = 8.85 \times 10^{-14} \text{ F/cm}$ , the input sensitivity,  $S1$ , is  $35.6 \text{ kV/cm} \cdot \text{V}$ . Thus, if  $V1 = 1 \text{ V}$ , then the electric field,  $E2$ , is  $35.6 \text{ kV/cm}$ .

Experimental results for the ELF sensor, shown in Fig. 6, were taken at room temperature and low temperature where the sensitivity is  $34.4 \text{ kV/cm} \cdot \text{V}$  at room temperature and  $65.1 \text{ kV/cm} \cdot \text{V}$  at  $-66.2^\circ\text{C}$ . This data can be analyzed using:

$$E2 = E20 + S1 \cdot V1 \quad (1)$$

where  $E20$  is the electric field at  $V1 = 0$ . The voltage intercept,  $V10 = -E20/S1$ . Representing the temperature dependence of  $E20$  and  $S1$  by  $E20 = E200 + KE(T - T0)$  and  $S1 = S10 + KS(T - T0)$  where  $KE$  and  $KS$  are coefficients of the temperature dependent terms,  $E200$  is the electric field at  $V1 = 0$  and  $T = 300\text{K}$ , and  $S10$  is the sensitivity at  $T = 300\text{K}$ . Combining the above equations leads to:

$$E2 = E200 + KE \cdot (T - T0) + S10 \cdot V1 + KS(T - T0)V1 \quad (2)$$

where  $T0$  is  $300\text{K}$  or  $26.85^\circ\text{C}$ . A least squares analysis of the data in Fig. 6 leads to  $E200 = -270.8 \text{ V/cm}$ ,  $KE = 2.85 \text{ V/cm} \cdot ^\circ\text{C}$ ,  $S10 = 34.14 \text{ kV/cm} \cdot \text{V}$ , and  $KS = -0.33 \text{ kV/cm} \cdot \text{V} \cdot ^\circ\text{C}$ . Using Eq. 2, the electric field is determined given  $V1$  and the temperature. Notice that  $S10$  ( $34.14 \text{ kV/cm} \cdot \text{V}$ ) determined from experimentation is close to the  $S1$  value derived above using component values ( $35.6 \text{ kV/cm} \cdot \text{V}$ ).

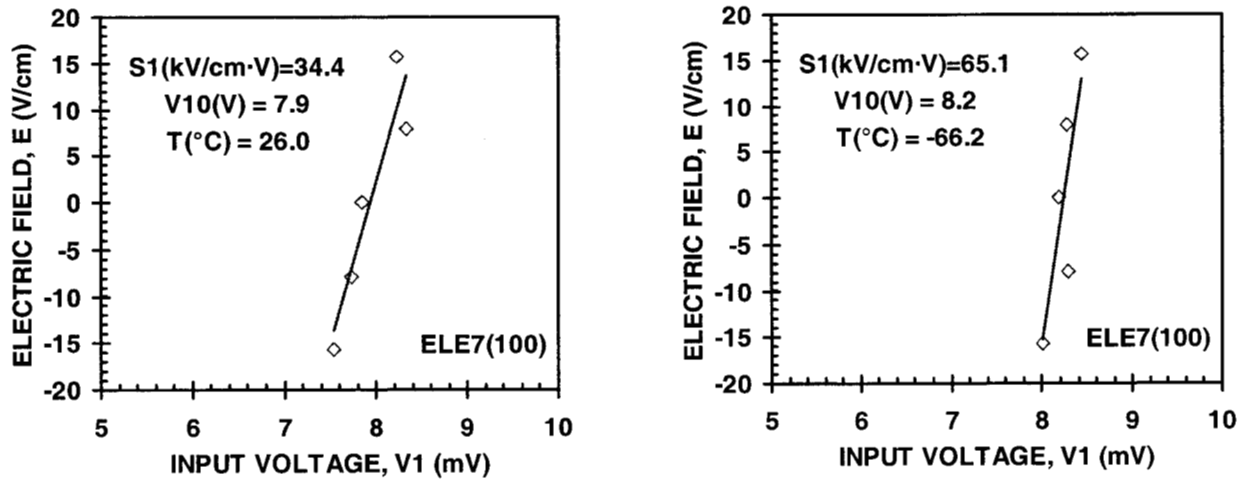


Figure 6. Room (left) and low (right) temperature response of the electric field monitor (ELF) where voltages are an average of 100 measurements. Signal averaging was necessary to increase the resolution of the 12-bit ADC from  $2 \text{ mV/bit}$  to  $0.2 \text{ mV/bit}$ .

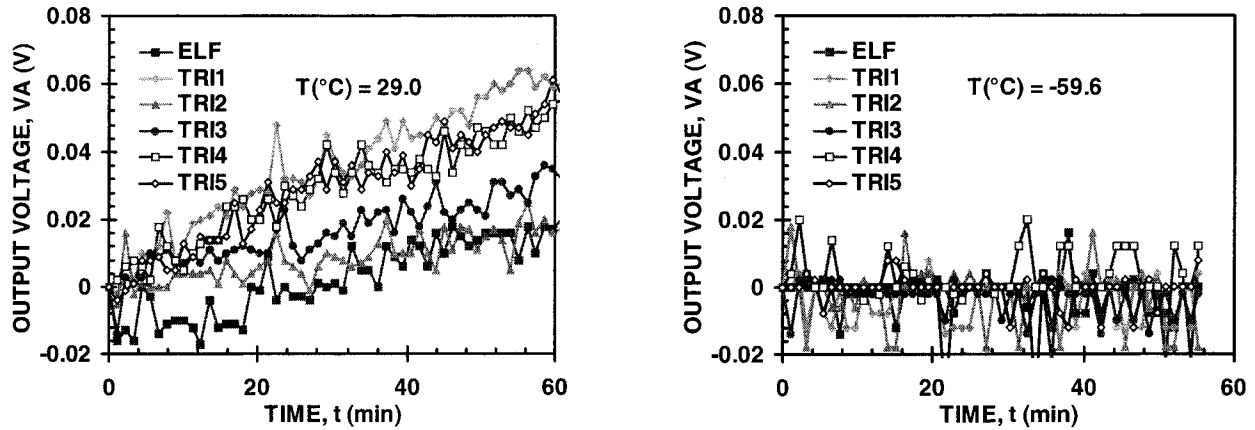


Figure 7. Room and low temperature voltage drift of the ELF and TRI sensors. At room temperature, the amplifier input voltage drift is between 1.25 and 4.5  $\mu\text{V}/\text{sec}$ .

This electrometer is an induction field meter [1] operated in a direct current mode, where the operational amplifier input current charges C1. For the operational amplifiers used in this circuit the input current is about 2 fA at room temperature. At lower temperatures, this value gets much smaller. The results in Fig.7 have the expected behavior. At room temperature the drift relative to the amplifier output is about 3  $\mu\text{V}/\text{sec}$  at room temperature (29.0°C) and essentially zero at the low temperature (-59.6°C). The data illustrates system noise which is related to the resolution of the 12-bit analog-to-digital converter which is 2 mV/bit.

**CIRCUIT DESIGN:** The electrical schematic of the electric field and triboelectric sensors is shown in Fig. 8. The design of the electric field sensor follows from the traditional electrometer [2]. The instrument is composed of a capacitive divider where C2 is the field sensing capacitor and C1 is the reference capacitor. The point between the capacitors is connected to the positive terminal of the first stage amplifier operated in the follower mode. The sensing electrode is protected by a driven guard that is connected to the negative terminal of the first stage amplifier. A second operational amplifier is added to provide additional amplification.

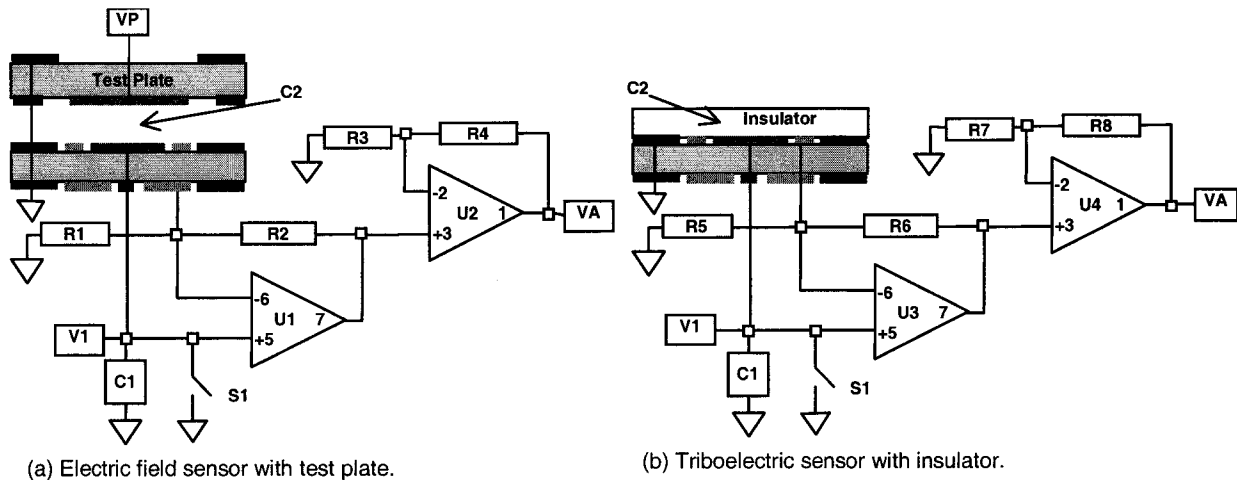


Figure 8. Schematic circuit representations for the (a) Electric field sensor (ELE) and (b) Triboelectric sensor (TRI).

At the beginning of the measurements, C1 is discharged using the solid-state switch, S1 which has very low leakage. In the ELF sensor, C2 has an air dielectric; whereas, in the TRI sensor, C2 has an insulator dielectric which acquires charge during rubbing. The ELF sensor was calibrated by placing various potentials, VP, on the test plate and recording the response at the amplifier output, VA. A similar test plate was used to calibrate the TRI sensor.

**SENSOR DESIGN:** The cross section of the electrometer is shown in Fig. 9. The design principle was based on the apparatus used at the Kennedy Space Center for characterizing the electrostatic properties of materials. In that apparatus samples are clamped into a 15-cm diameter holder that grounds the periphery of the sample. Thus, after rubbing, samples are characterized by the rate of charge leakage to the ground ring. These features are replicated in miniature as seen in Fig. 9.

To characterize antistatic materials, an insulator sandwich is created as shown in Fig. 9. The antistatic film insulator is laid on top of a bulk insulator and clamped in place under the ground ring.

The assembly is designed so that the insulators can be replaced by removing the fasteners that consist of non magnetic stainless steel screws. The use of nonmagnetic screws is important since a major constituent of the Martian regolith is Hematite ( $\text{Fe}_2\text{O}_3$ ) which is magnetic. To be in compliance with planetary protection, the cavity is sealed with epoxy.

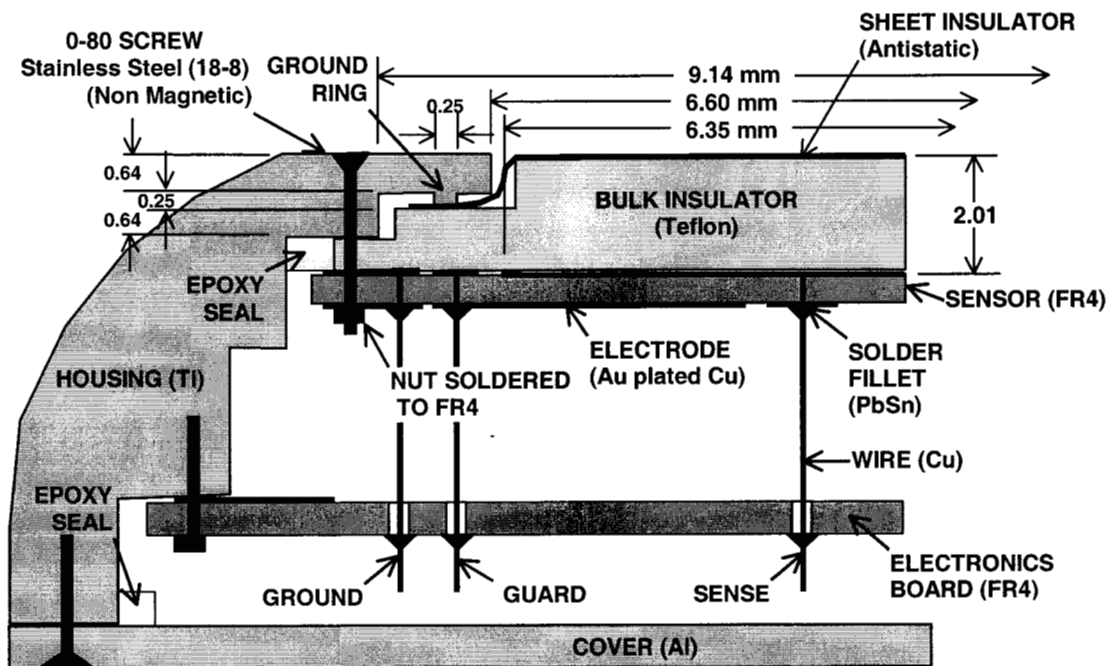


Figure 9. Partial cross section of the electrometer showing the sensor and insulator sandwich and their connection to the electronics board.

**EXPERIMENTS:** Four different insulating materials were loaded into the titanium triboelectric sensor head and manually rubbed at room temperature with wool felt; the results are shown in Fig. 10. The falling response between 40 and 50 seconds represents the rubbing period. The

curves then tend to zero after a period that exceeds 100 s. The large negative response is for the teflon which is to be expected for teflon rubbed on wool.

The results in Fig.10, can be related to the electric field using Eq. 2. For this analysis the amplifier output at  $V_A = 0.4$  V was chosen. First,  $V_1$  was determined using  $V_A$  and the amplifier gain,  $G = 4$ . Then, Eq. 2 was evaluated using  $T = 27.5$  °C and  $V_1 = 0.1$  V and the electric field calculated as  $E_2 = -3.7$  kV/cm.

The curves shown in Fig. 10 are encouraging in that they indicate that the electrometer signal is substantial, being in the 100 mV range. The signals are much larger than the millivolt signals measured during the calibration as depicted in Figs. 6 and 7. This means that the drift in the input voltage, as seen in Fig. 7, are not of concern for measurements taken at or below room temperature for times on the order of 10 seconds.

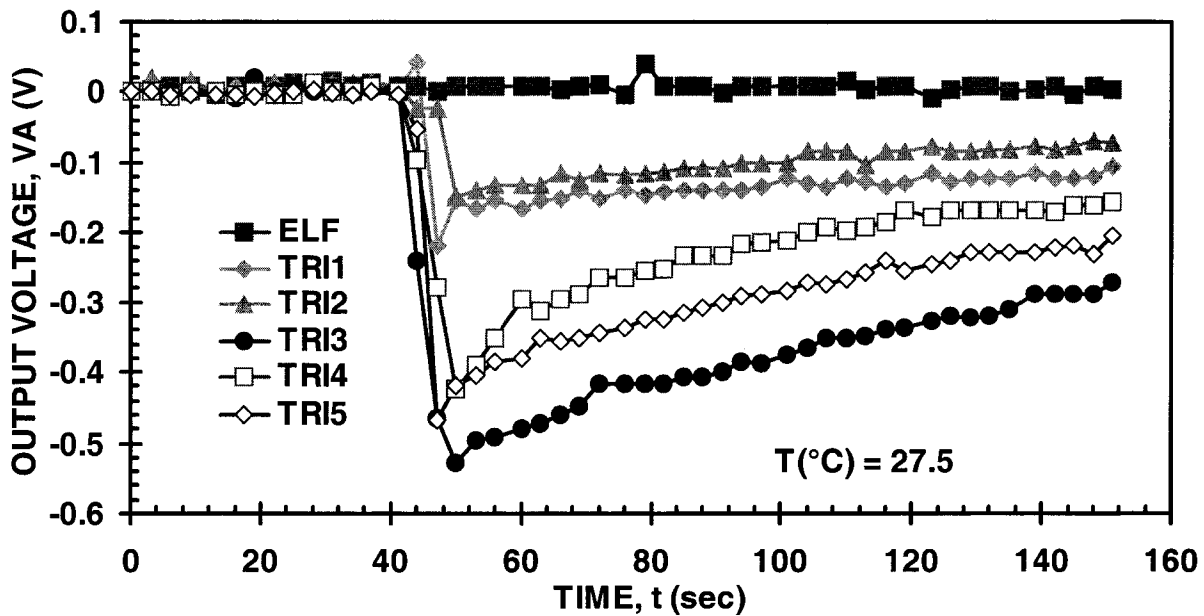


Figure 10. Response of triboelectric sensors after being rubbed with wool felt where TRI1 is ABS, TRI2 is polycarbonate, TRI3 is Teflon, TRI4 is Rulon-J, and TRI5 is Teflon.

**DISCUSSION:** At this time, the flight units are under construction and the measurements presented here are from a prototype unit termed ELE7. The final selection of insulating materials will be done in the next few months. It is anticipated that dust cling to the insulator surface will affect the results in that the dust will compensate the triboelectrically induced charge in the insulator thus reducing the response. In the next few months, tests will be performed to quantify this effect and procedures sought to remove the dust.

#### REFERENCE:

1. J. A. Cross, "Electrostatics: Principles, Problems and Applications", Adam Hilger (Bristol, UK)
2. "Electrometer Measurements", Keithley Instruments (Cleveland OH, 1972).

**ACKNOWLEDGMENTS:** The work described in this paper was performed by the Jet Propulsion Laboratory, California Institute of Technology, under a contract with the National Aeronautics and Space Administration. The authors are indebted to the managers who have encouraged this work. In particular from JPL, Michael Hecht, Lynne Cooper, and Joel Rademacher, from WVU, Tom Meloy, and from KSC Haesoo Kim and Rupert Lee.

In addition the authors appreciate the efforts of the MECA/Electrometer science advisor board that was convened at Electrostatics '99. The board has provided guidance and a number of important suggestions. The board members and their affiliations are: Peter Castle, University of Western Ontario, Jon Chubb, John Chubb Instrumentation, Michael Dyer, Du Pont, William Greason, University of Western Ontario, Paul Holdstock, British Textile Technology Group, Thomas Jones, University of Rochester, Z. Kucеровsky, University of Western Ontario, and David Swenson, EDS Association. File: Camb9516.doc.